Aerosol Forecasts by Eta-CMAQ for the poor air quality episode in early February 2005

Pius Lee [*1,2], Jeffery McQueen[2], Rohit Mathur[3], Marina Tsidulko[1,2], Shobha Kondragunta[4], Jon Pleim[3], Daiwen Kang[3,5], Hsin-Mu Lin[3,5], Tanya Otte[3], Jeff Joung[3], George Pouliot[3], Geoff DiMego[2], Ken Schere[3], Paula Davidson[6] and Nelson Seaman[6]

1. INTRODUCTION

Many air pollution agencies in the Upper Midwest and the Great Lakes regions had issued air advisories between January 31st and February 4th, 2005. Air Quality Index (AQI) issued on the EPA web site for Minnesota peaked at 155 on January 31st. In the Chicago area, AQI measured between 110 and 140 for most of this first week of February. The deterioration of the air quality over these regions for a rather prolonged duration had been attributed to the slow passing of broad high pressure systems centered over the Great Lakes during the period. The pressure systems were accompanied by extensive cloudiness and snow coverage over the same regions. This combination of meteorological conditions resulted in reduced atmospheric mixing; and high rates of atmospheric particle formation and growth due to high RH in the lower levels.

In this study, the National Weather Service's (NWS) Eta-CMAQ (Rogers et al, 1996, Bynn and Ching, 1999) Air Quality Forecast System (AQFS) (Otte et al, 2005, Davidson et al, 2004) has been used in a research mode to predict the aerosol concentration and speciation of this poor air episode. The model result has been verified in a crude manner by comparing its Aerosol Optical Depth (AOD) prediction with that observed by the Geostationary Operational Environmental Satellites (GOES) (NOAA, 2005a-b), and surface level aerosol concentration prediction with that compiled by the Aerometric Information Retrieval Now (AIRNOW) (EPA, 2005) observation network.

2. DERIVING PM2.5 AND AOD

The aerosol module in CMAQ adopts a modal approach to represent the particles suspended in air (Binkowski and Roselle, 2003; Mebust et al, 2003). It uses the superposition of 3 log-normal sub-distributions to represent the size distribution of these particles. Fine particles with diameter less than 2.5 μm (PM2.5) are represented by two of these sub-distributions called the Aitken (i), particles have diameters up to 0.1 μm, and the accumulation (j), particles have diameters between 0.1 and 2.5 μm, modes. Table 1 shows the speciation of the particles in the i and j modes. The i mode particles usually represent particles freshly formed from nucleation or from direct emission, whereas the larger j mode particles represents aged particles. The chemical species treated in these modes are also tabulated in Table 1.

The model treats the interaction between these fine modes and the coarse mode in a one-way merging manner into the coarse mode, when the fine modes particles grow beyond 2.5 μm in diameter. However, there is no implementation of coagulation between the fine modes and the coarse mode.

*Corresponding Author Address: Pius Lee, EMC/NCEP, W/NP22 Room 207, 5200 Auth Road, Camp Springs, MD 20746-4304
pius.lee @noaa.gov
[1] Scientific Applications International Corporation, Beltsville, M
[2] Environmental Modeling Center, NOAA/NWS/NCEP, Camp Springs, MD
[3] National Oceanic and Atmospheric Administration, Research Triangle Park, NC (On assignment to the National Exposure Research Laboratory, US EPA)
[4] National Environmental Satellite and Data Information Service, Camp Springs, MD
[5] Science and Technology Corp., Research Triangle Park, NC
[6] Office of Science and Technology, NWS, Silver Spring, MD

Table 1. Speciation and variable name used in the CMAQ aerosol module

Species description	Name
Accumulation mode sulfate mass	ASO4J
Aitken mode sulfate mass	ASO4I
Accumulation mode ammonium mass	ANH4J
Aitken mode ammonium mass	ANH4I
Accumulation mode nitrate mass	ANO3J
Aitken mode nitrate mass	ANO3I
Accumulation mode anthropogenic secondary organic mass	AORGAJ
Aitken mode anthropogenic secondary organic mass	AORGAI
Accumulation mode primary organic mass	AORGPAJ
Aitken mode primary organic mass	AORGPAI
Accumulation mode secondary biogenic organic mass	AORGBJ
Aitken mode secondary biogenic organic mass	AORGBI
Accumulation mode elemental carbon mass	ACEJ
Aitken mode elemental carbon mass	ACEI
Accumulation mode unspecified anthropogenic mass	A25J
Aitken mode unspecified anthropogenic mass	A25I
Accumulation mode water mass	AH2OJ
Aitken mode water mass	AH2OI

The coarse mode modeling has not been emphasized due to the large uncertainty in the determination of its emissions. Furthermore in terms of health hazard considerations, the finer 2 modes are of more concern. Subsequently, in the model PM2.5 concentration at the surface level is derived by summing up all those concentrations pertaining to the species listed in Table 1. By the same token, the current CMAQ model does not include coarse mode particles in its visual range calculations. Therefore the AOD calculation outlined below does not account for the effect of coarse mode particles. AOD, a dimensionless quantification of visibility impairment, is defined in the following equation.

$$AOD = \int_{0}^{ModelTop} B_{sp} \quad dz \qquad (1)$$

Where B_{sp} is the aerosol extinction coefficient in km^{-1}, z is altitude in km. CMAQ calculates B_{sp} through Q_{ext}, the extinction efficiency, a measure of light scattering efficiency which in turn is estimated using approximations to the Mie theory (Binkowski, 1999):

$$B_{sp} = \frac{3\pi}{2\lambda} \int_{-\infty}^{\infty} \frac{Q_{ext}}{\alpha} \frac{dV}{d\ln\alpha} d\ln\alpha \qquad (2)$$

Where $\alpha = \pi D / \lambda$, D is the particle diameter, V is the volume of the particle, and λ is the wavelength of the incident light.

3. METEOROLOGY OF JANUARY 31 & FEBRUARY 1. 2005

On both days of January 31st and February 1st, 2005, moderate to weak high pressure systems dominated much of the continental U.S as shown in Figs. 1a and 1b. There were essentially three large high pressure systems that together covered much of the mid to northern parts of the continental U.S. The high pressure system in the middle, which located over the Midwest and the Great Lakes, was the weakest and the fastest moving among the systems. In contrast with the other two stronger systems, which happened to be more stationary on other sides, this system in the middle experienced more cloudiness as it passed southward. The weak pressure gradients and the generally fair weather condition there rendered the air mass calm and stagnant. Satellite images of those days, as shown in Figs. 2c and 3c, illustrated the cloudiness condition over the Midwest areas during those days.

Over the Upper Midwest and the Great Lakes, snow cover was prevalent, and the surface level air temperature in those areas varied between -5°C and 5°C during the period. These temperatures and the abundance of water vapor fed from the melting and sublimating snow provided a favorable condition for fog and hydroscopic aerosol particles to grow. Consequently, low clouds and fog further inhibited mixing activities in the lower atmosphere. This compounded condition of stagnant air, low cloud and rather warm temperature around the freezing point gave rise to heavy suspension of fog and aerosol particles

in the lower atmosphere in the area for a prolonged period of time during those days.

4. VERIFICATION OF AOD AND PM2.5

Figures 2b and 3b show the model predicted AOD and surface level PM2.5 concentration. The shaded fields, using the side color bar color code, depict the dimensionless AOD field. It was obtained by evaluating Equations (2) and (1) through the use of predicted instantaneous aerosol concentrations. The colored line contours depict PM2.5 concentrations in μgm^{-3}.

To evaluate the model predicted AOD against observation we have used AOD values compiled basing on imageries obtained by the GOES satellites. The time resolution of the satellite data retrieval is 30 minutes. Cloudiness can however deprive the opportunity of the AOD data compilation. A more resilient verification method by using the Moderate Resolution Imaging Spectroradiometer (MODIS) (IDEA, 2005) satellites which are able to distinguish between aerosol and cloud optical depths is currently under development at NCEP.

In Figs. 2b and 3b there showed high predicted values of AOD in the upper Midwest areas in the afternoons of both January 31st and February 1st, 2005 respectively. In Fig. 2b there also showed high predicted values of AOD around the southeastern Louisiana area on January 31st. Nonetheless, all these aforementioned areas were under clouds for most of these days rendering no AOD observation data compilation from the GOES satellites. For the clear sky areas shown on the satellite imagery in Fig. 2c for January 31st, such as areas along the U.S. Eastern Seaboard, the observed AOD ranged between 0.2 and 0.3, whereas there were a few spotty high values above 1.0. They agreed rather well with those model predicted values shown in the corresponding areas in Fig. 2b. However, agreement for the high observed AOD values offshore the Floridian Pam Handle is not good as shown in Figs. 2b and 2c. On February 1st, this agreement offshore the Floridian Pam Handle improved as shown in Figs. 3b and 3c. There was a belt of clear sky areas extending from the middle of Missouri to Northern Virginia and looped around to northeastern Georgia. The observed and the predicted AOD agreed quite well in this stretch of sunny regions during the afternoon of February 1st as shown in Figs. 2b and 2c.

In terms of verification of the prediction of surface PM2.5 aerosol concentration, the AIRNOW compiled values have been used as shown in Figs. 2a and 3a for the respective days. Figure 2b shows a cluster of high predicted surface PM2.5 concentration equals to or larger than 35 μgm^{-3} for most of Ohio and Indiana on January 31st. There were also shown 2 tongues of contours for values between 30 - 35 μgm^{-3} extended from these states to southern Michigan and eastern Minnesota respectively. The concentration levels of 15 - 20 μgm^{-3} were also shown along the U.S. Eastern Seaboard in Fig. 2b. These 3 features were roughly reflected by the AIRNOW observations as shown in Fig. 2a. In the afternoon of February 1st, the model predicted a cluster of high surface PM2.5 concentration equals to or larger than 35 μgm^{-3} expanded southwards reaching northern Oklahoma as shown in Fig. 3b. It also shows that the concentration level in the Boston-Philadelphia corridor increased to 30 - 35 μgm^{-3}. These two changes were reflected by the AIRNOW observations shown in Fig. 3a.

5. PREDICTED CONCENTRATION FIELDS

Speciation and spatial distribution of the aerosol species is only available from the predicted results. These two aspects of model fidelity can be occasionally verified when comprehensive data sets of large field campaign endeavored to make these data available. A case in point is the International Consortium for Atmospheric Research on Transformation and Transport (ICARTT) of July – August 2004 (ICARTT, 2005).

Figures 4a - 4d show surface concentration of gaseous NO_x ($NO+NO_2$), SO_4^{-2}, NO_3^{-1}, and organic aerosols respectively. From the Figs. 4a and 4d, it is noticeable that the spatial distribution of NO_3^{-1} mirrors closely that of NO_x, its precursor. Basing on Figs. 4b and 4c, one may conclude that the bad air quality episode in the surface levels in the afternoon of February 1st, 2005, was largely an inorganic event with SO_4^{-2}, NO_3^{-1} aerosols being the dominating surface aerosol species. It may also be inferred from the rather low concentration of NH_4^{+1} relative to that of NO_3^{-1} that it was a non-agricultural event as shown in its vertical profiles throughout the region of interest; namely in Figs. 5–9 for Cedar Rapids, St. Paul, Milwaukee, and two locations in Chicago respectively. The

generally high surface level concentration of anthropogenic mass is further indicative that industrial activities were among the main sources of pollutant emission as shown in Figs. 5-9.

The vertical profiles of NO_x and NO_3^{-1} follow one another closely as shown in Figs. 5-9. Similar precursor and product relationship can also be said to be true between SO_2 and SO_4^{-2}. The profiles of NH_3 and NH_4^{+1} are however rather different due to the short life time of the former relative to that of the latter.

The vertical concentration profiles of O3 and NO_x almost crisscrossed one another always vertically at all sites. This characteristic of the profiles of the two species were especially noticeable at night and in the early morning when O3 is titrated by NO_x. Figure 9 refers to a site in Lake Michigan a few miles offshore the city of Chicago. Ozone titration did not occur there as there was little local NO_X emission. However, the degree of pollution in terms of SO_4^{-2}, NO_3^{-1} was still considerable due to transport of pollutants from the city. Peculiarly the aerosols' water content at this offshore site is the lowest among all the sites shown in Figs. 5-9. It was due to the fact that relative humidity over that part of the lake, which was frozen on the surface, was lower than those over land during much of those two warm winter days in the region.

The O'Hare site was perennially laden with a high emission of NO_x as shown in Fig. 8. This NO_x rich air mass around the O'Hare site was probably due to the high temperature combustion exhaust from the taking-off and landing airplanes at around O'Hare Airport.

6. ACKNOWLEDGEMENT AND DISCLAIMER

The views expressed are those of the authors and do not necessarily represent those of NOAA or the EPA. The EPA AIRNOW program staff provided the observations necessary for quantitative model evaluation.

Disclaimer: The research presented here was performed under the Memorandum of Understanding between the U.S. Environmental Protection Agency (EPA) and the U.S. Department of Commerce's National Oceanic and Atmospheric Administration (NOAA) and under agreement number DW13921548. Although it has been reviewed by EPA and NOAA and approved for publication, it does not necessarily reflect their policies or views.

7. References

Binkowski, F. S. and S. J. Roselle, 2003: Models-3 Community Mutliscale Air Quality (CMAQ) model aerosol component: 1: Model description, *J. Geophys. Res.*, **108**(D6), 4183, doi:10.1029/2001JD001409,2003.

Binkowski, F. S., 1999: The aerosol portion of Models-3 CMAQ, in *Science Algorithm of the EPA Models-3 CMAQ Modeling System*, edited by D.W. Byun and J.K.S. Ching, Rep. EPA-600/R-99/030, pp 1-23.

Byun, D. W., and J. K. S. Ching (Eds.), 1999: *Science algorithms of the EPA Models-3 Community Multiscale Air Quality (CMAQ) Modeling System*. EPA-600/R-99/030, Office of Research and Development, U.S. Environmental Protection Agency, Washington, D.C. [Available from U.S. EPA, ORD, Washington, D.C. 20460.]

Davidson, P. M., N. Seaman, K. Schere, R. A. Wayland, J. L. Hayes, and K. F. Carey, 2004: National air quality forecasting capability: First steps toward implementation. Preprints, *Sixth Conf. on Atmos. Chem.*, Amer. Met. Soc., Seattle, WA, 12-16 Jan 2004.

EPA 2005: AIRNOW Network [Available at http://www.epa.gov/airnow]

ICARTT, 2005: [Available at http://www.al.noaa.gov/metproducts/icartt04/]

IDEA, 2005: Infusing Satellite Data into Environmental Applications, [Available at http://idea.ssec.wisc.edu/index.php]

Mebust, M. R., B. K. Eder, F. S. Binkowski and S. J. Roselle, 2003: Models-3 Community Mutliscale Air Quality (CMAQ) model aerosol component: 2: Model evaluation, *J. Geophys. Res.*, **108**(D6), 4184, doi:10.1029/2001JD001410, 2003.

NOAA, 2005a: National Environmental Satellite, GOES aerosol and SMOKE Product. [Available at http://www.gis.ssd.nesdis.noaa.gov/GASP, and http://lwf.ncdc.noaa.gov/oa/climate/research/2005/fire05.html]

NOAA, 2005b: Satellite Service Division and Fire Detection Program. [Available at http://www.ssd.noaa.gov/PS/FIRE/hms.html]

Otte, T.L., G. Pouliot, J. E. Pleim, J. O. Young, K. L. Schere, D. C. Wong, P. C. S. Lee, M. Tsidulko, J. T. McQueen, P. Davidson, R. Mathur, H.Y. Chuang, G. DiMego, and N. L. Seaman, 2005: Linking the Eta model with the Community Multiscale Air Quality (CMAQ) modeling system to build a national air quality forecasting system, *Wea. Forecasting*, **20** (No.3), 367–384.

Rogers, E., T. Black, D. Deaven, G. DiMego, Q. Zhao, M. Baldwin, N. Junker, and Y. Lin, 1996: Changes to the operational "early" Eta Analysis / Forecast System at the National Centers for Environmental Prediction. *Wea. Forecasting*, **11**, 391-413.

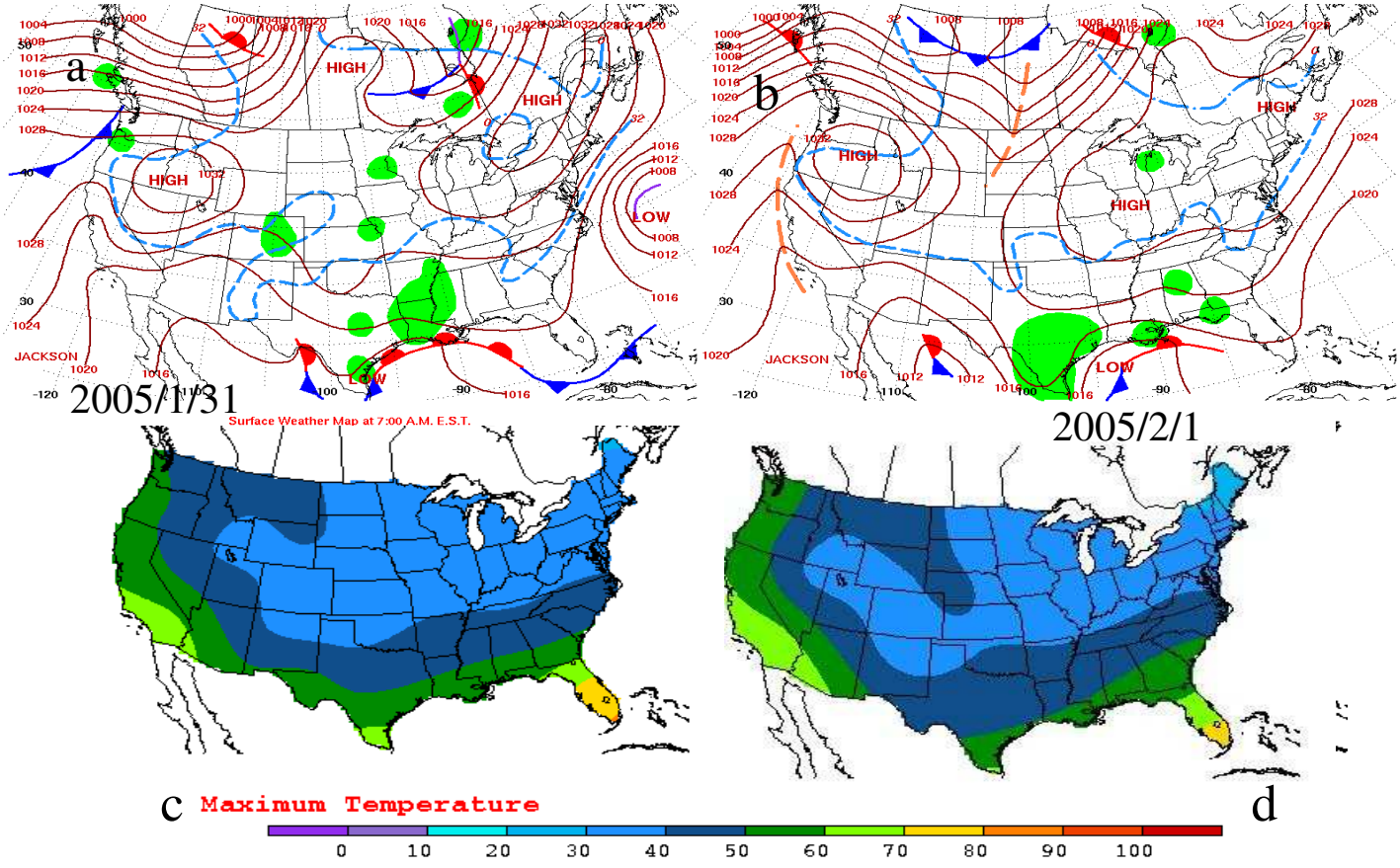

Figure 1: Surface weather map: (a) for January 31st and (b) for February 1st 2005. Surface daily maximum temperature: (c) for January 31st and (d) for February 1st 2005.

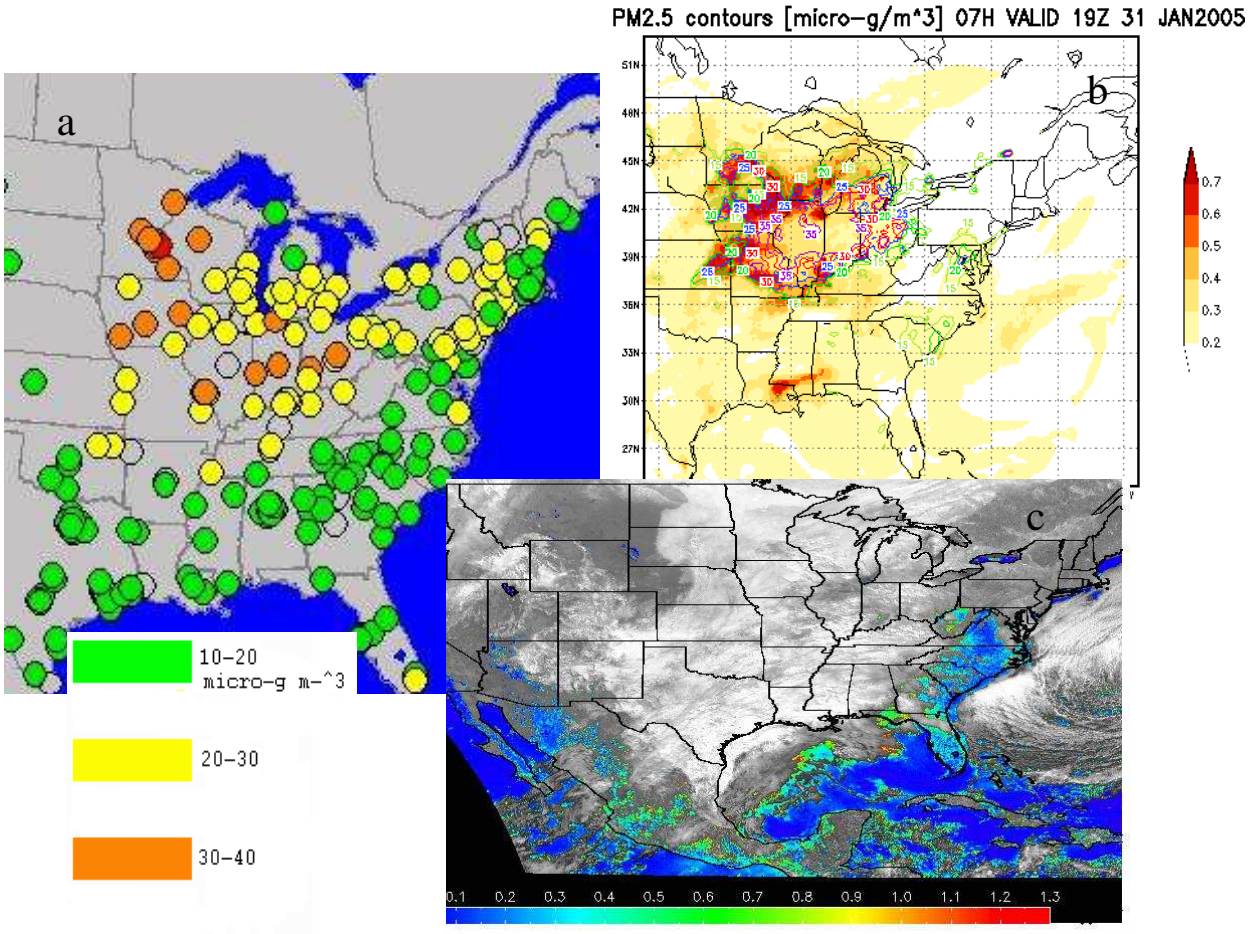

Figure 2: Predicted and observed column total AOD and surface level PM2.5 values valid at around 19 UTC January 1st, 2005: (a) Observed PM2.5 by the AIRNOW network where green, yellow and orange data points represent concentration between 10 and 20; between 20 and 30; and between 30 and 40 μg m^{-3} respectively, (b) predicted column total AOD, color shaded in accordance with the side color bar; and PM2.5, colored contour lines with labels: light green for 15, dark green for 20, blue for 25, red for 30, and purple for 35 μg m^{-3} respectively, and (c) GOES imagery on AOD with cloud.

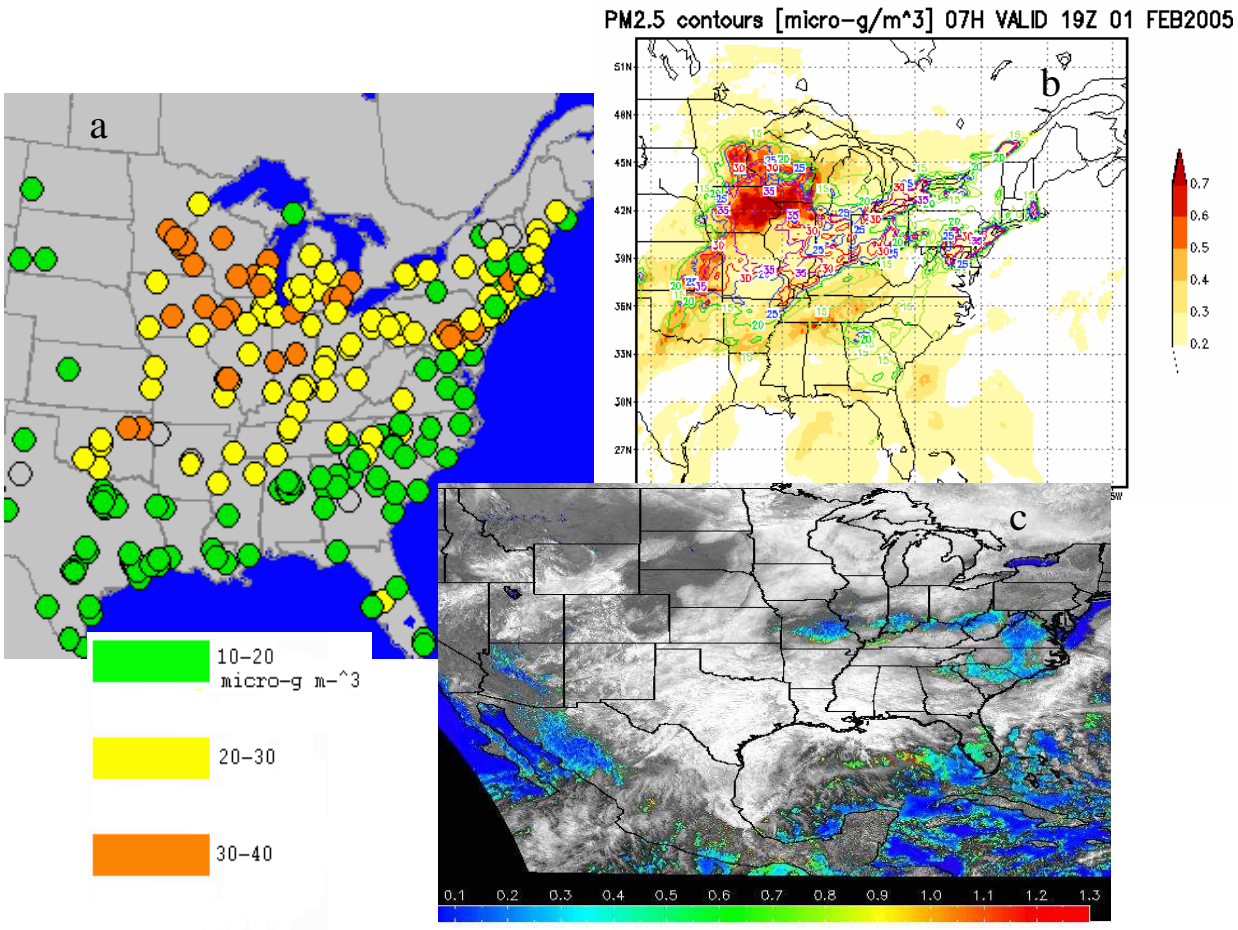

Figure 3: Same as Fig. 2 but for February 1st, 2005.

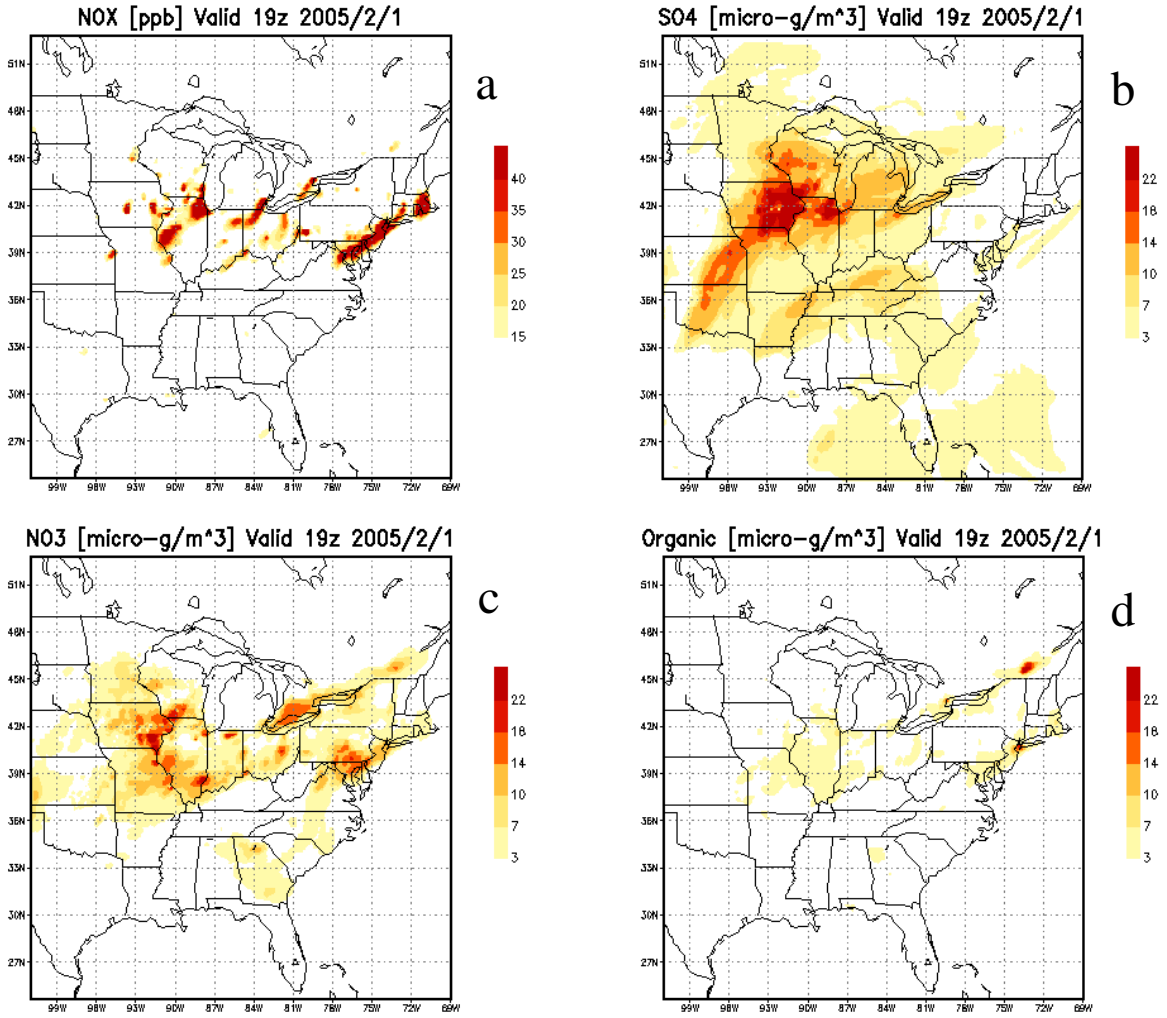

Figure 4: Predicted concentration of chemical species valid at 19 UTC February 1st, 2005: (a) for NO_x ($NO+NO_2$), (b) SO_4^{2-}, (c) NO_3^-, and (d) Organic aerosols.

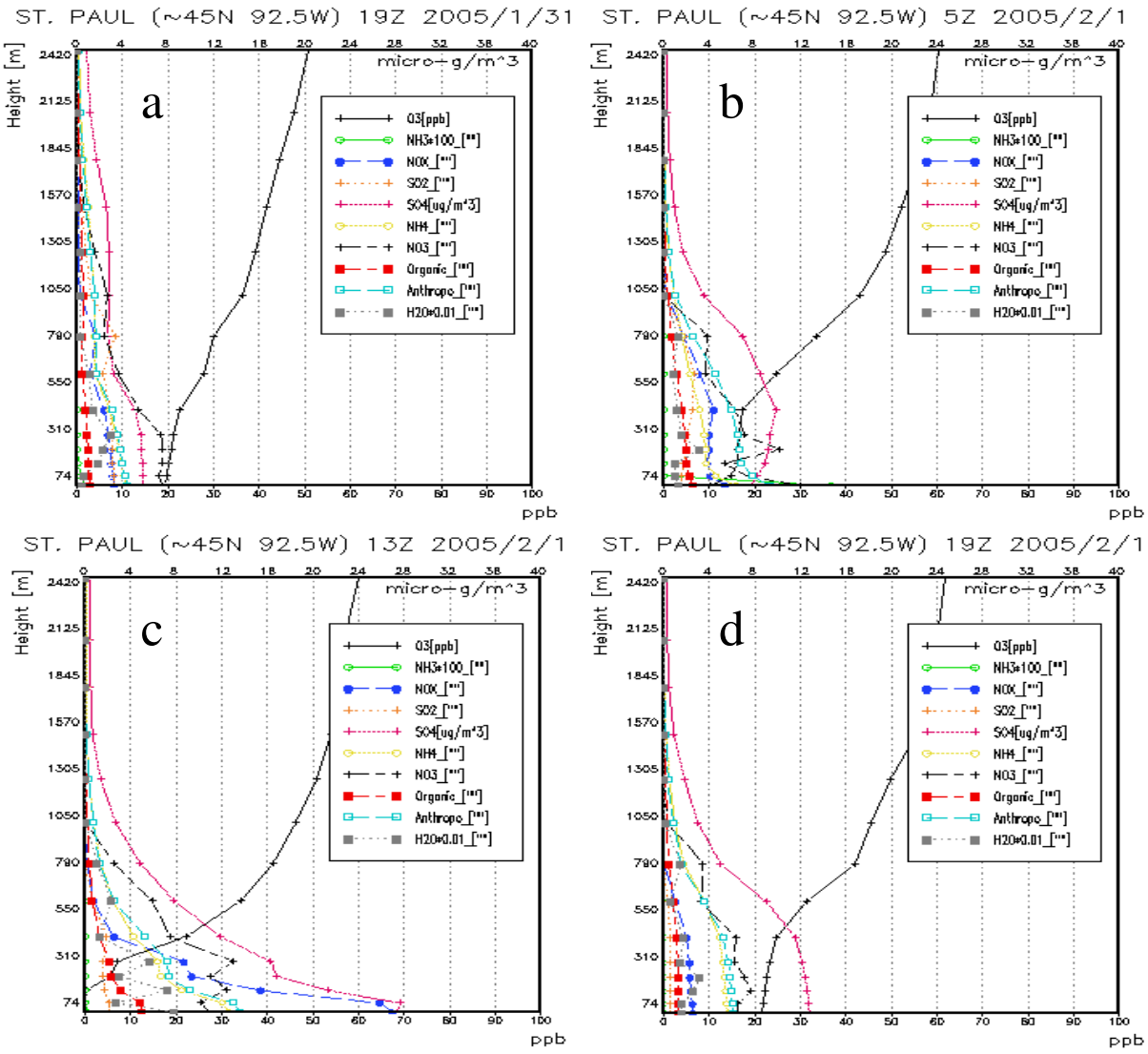

Figure 5: Predicted vertical concentration profiles at St. Paul, WI, for species aforementioned in the order from top to bottom in the legend boxes; for gaseous species in ppb: O_3, NH_3 (magnified 100 times), NO_X, and SO_2; and for aerosol masses in μg m^{-3}: SO_4^{2-}, NH_4^+, NO_3^-, organic, anthropogenic, and water content at (a) 19 UTC January 31st, (b) 5 UTC February 1st, (c) 13z February 1st, and (d) 19 UTC February 1st, 2005.

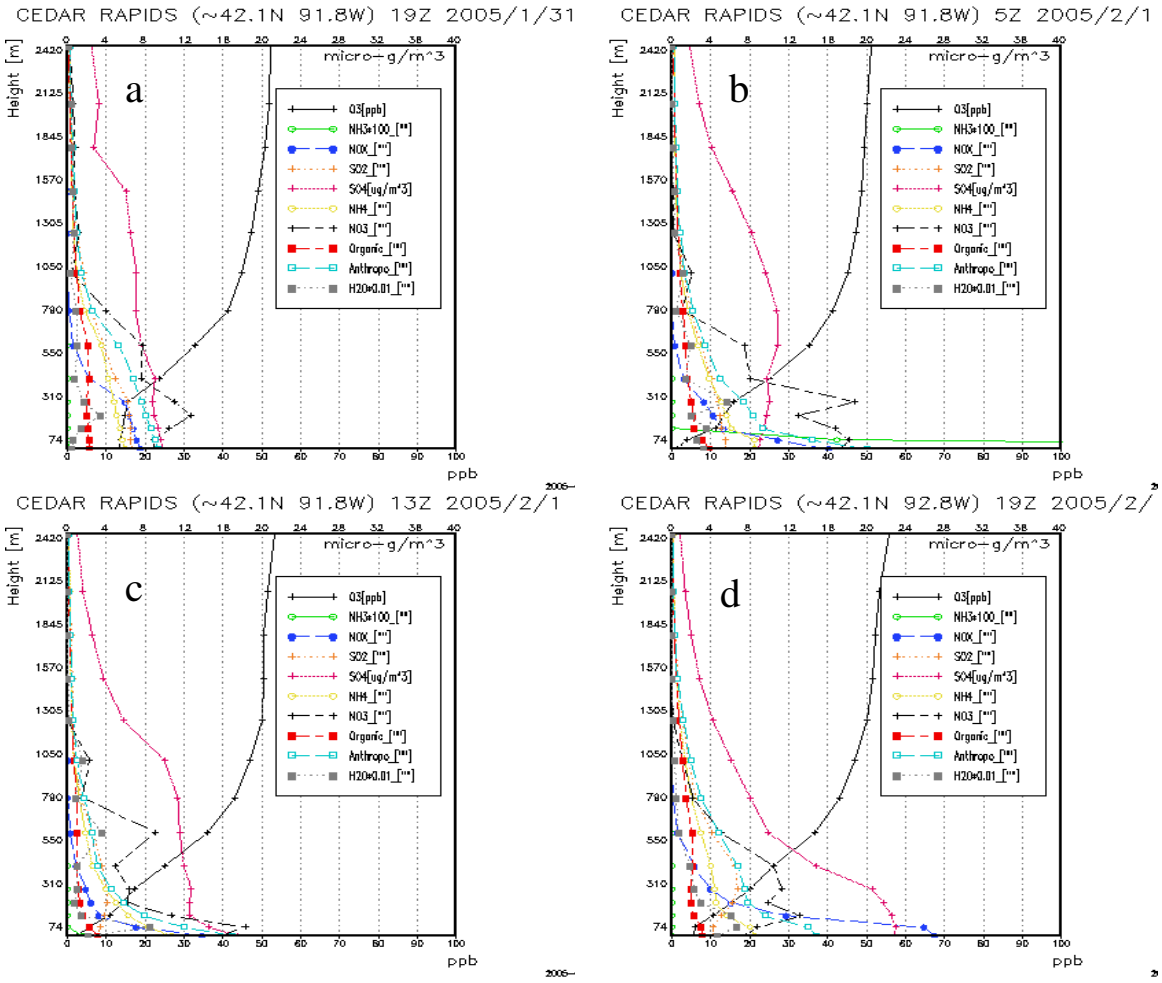

Figure 6: Same as Fig. 5 but for Cedar Rapids, IO.

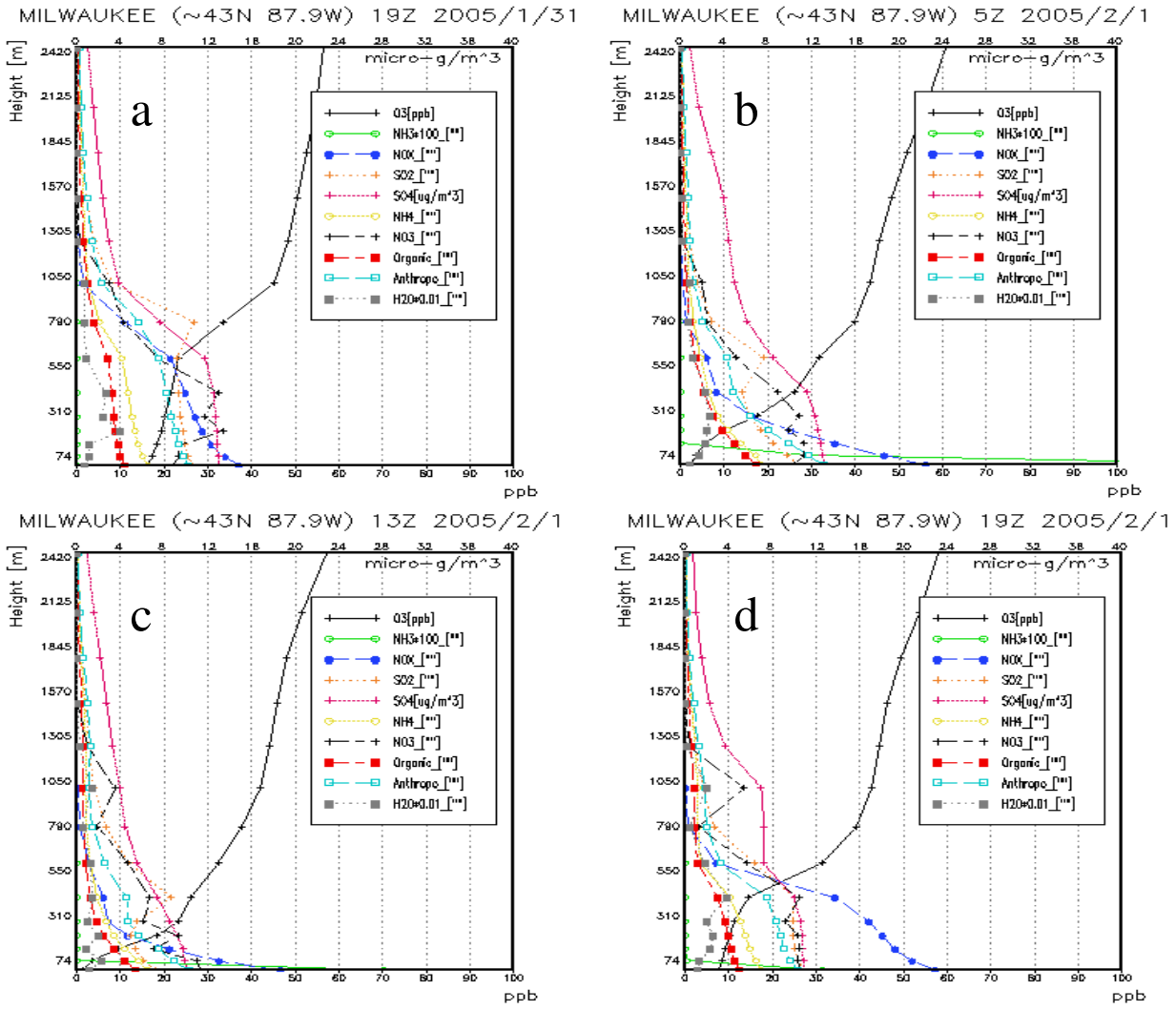

Figure 7: Same as Fig. 5 but for Milwaukee, WI.

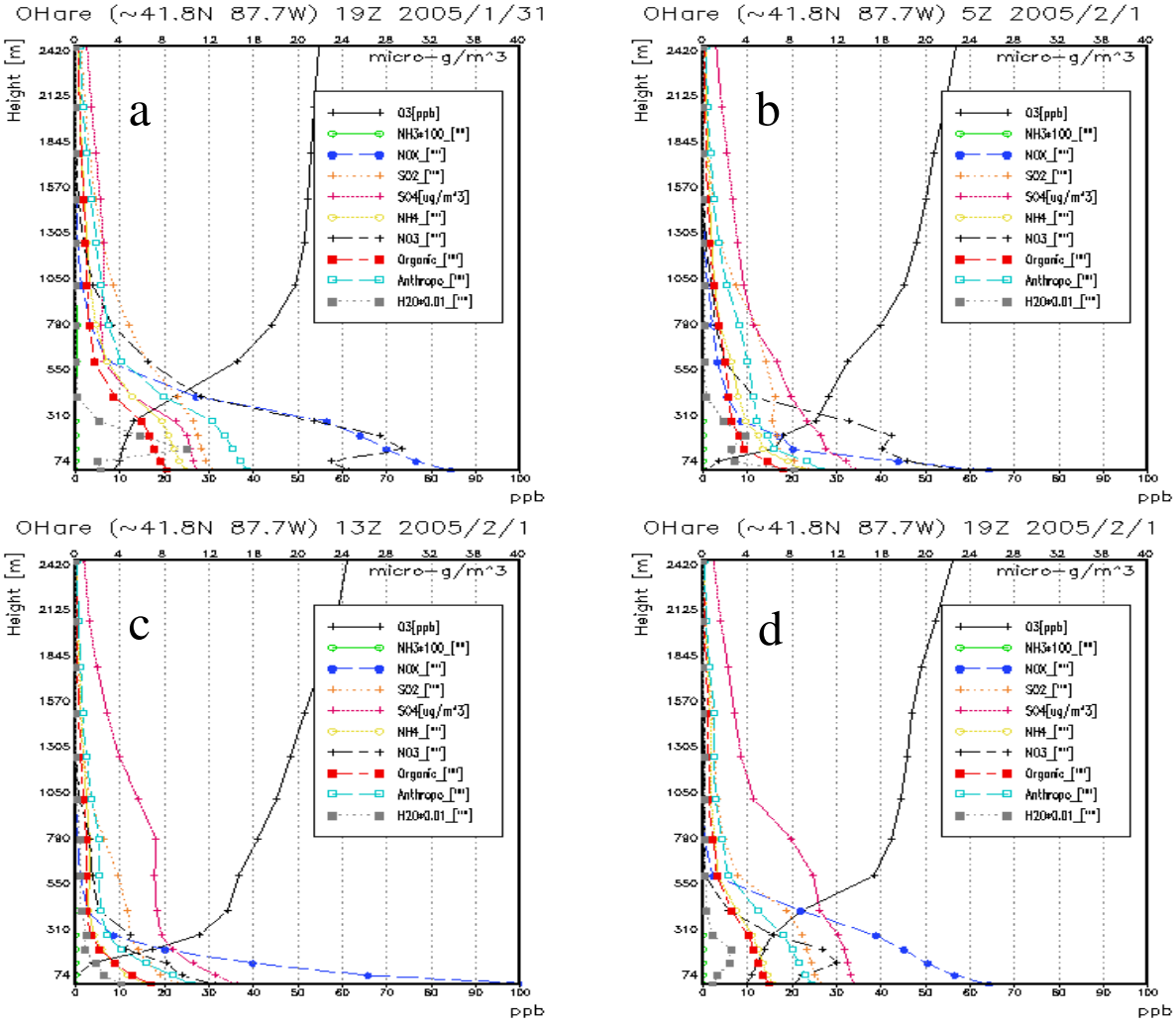

Figure 8: Same as Fig. 5 but for O'Hare Airport, Chicago, IL.

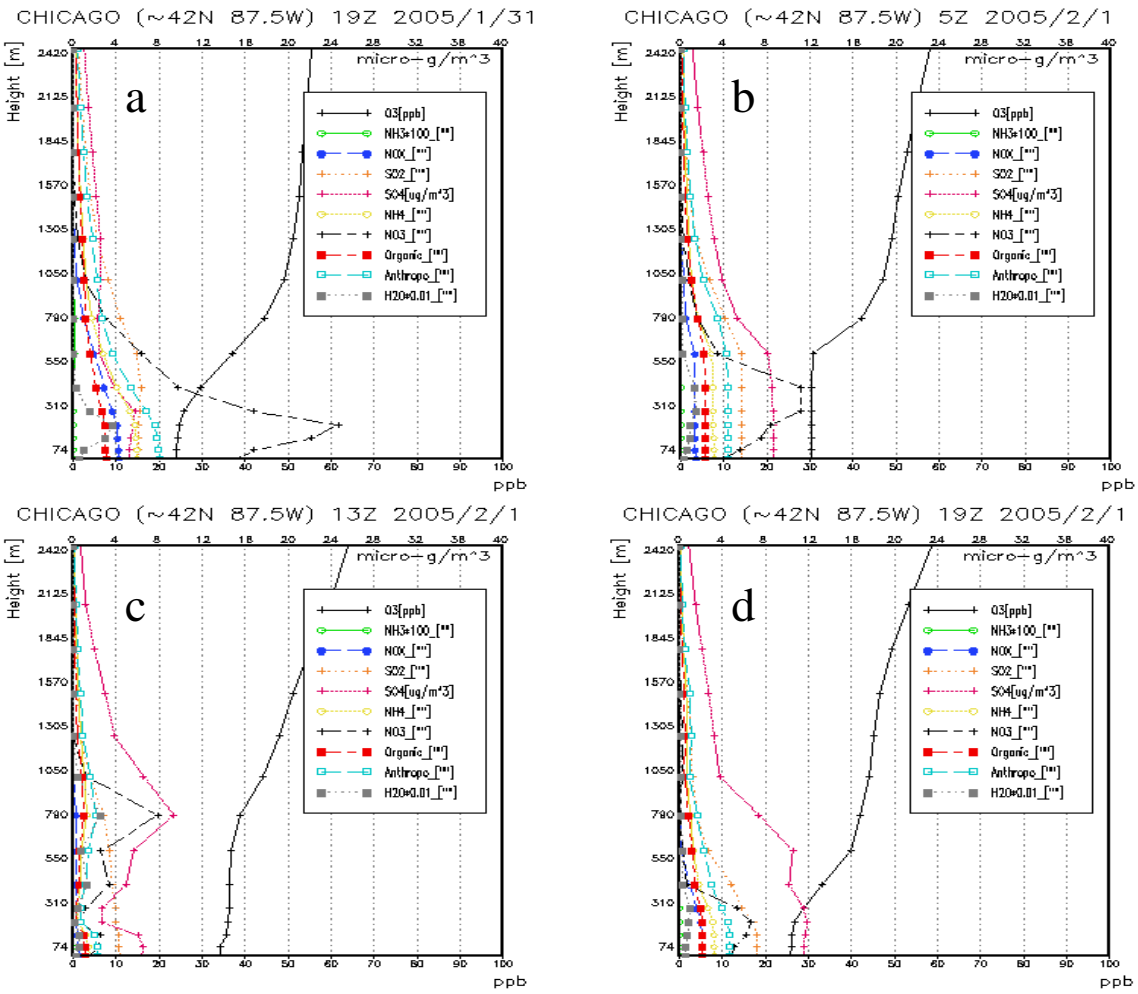

Figure 9: Same as Fig. 5 but for a site in Lake Michigan just offshore, Chicago, IL.